Journal of Information and Computing Science
J. Info. Comput. Sci., Vol. 18, No. 2, pp. 129-140

DOI: 10.4208/JICS-2023-009
December 2023

Solving surface potential of DC grounding electrode by Chebyshev polynomial

Huanruo Qi[1,*], Chen Chen[1], Xiangyang Yan[1], Yilong Kang[1], Shunran Wang[1] and Xu Diao[1]

[1] *Economic and Technological Research Institute of State Grid Henan Electric Power Company, Zhengzhou 450052, China*

Abstract. The operation experiences have shown that the large-scale DC magnetic bias caused by DC grounding electrode can be attributed to the uneven surface potential distribution. Here, the Chebyshev polynomial is used to fit the Hankel transform kernel function in order to solve the surface potential distribution for the complex earth model of wide area depth stratification. The adaptive order fitting method of Chebyshev polynomial for kernel function is obtained via shift operation, coefficient expansion and truncation error determination, which greatly reduces the calculation difficulty of surface potential distribution in a large area caused by DC grounding electrode. Compared with the standard grounding calculation software CDEGS, the proposed Chebyshev polynomial approach achieves less than 1 V of earth surface potential deviation in range of 1-100 km when the DC grounding current is 5 000 A. Moreover, the order of the Chebyshev polynomial has influence on the solution results, and it is confirmed that the 20th-order Chebyshev polynomial can meet the accuracy requirements for general DC bias risk assessment. The proposed surface potential assessment method based on shifted Chebyshev polynomial provides a basic technical means for the risk assessment of DC bias, which is helpful to reduce the difficulty of DC bias risk assessment for power grid.

AMS subject classifications: 41A50, 76B07

Key words: DC grounding electrode, Surface potential, Chebyshev polynomial, Hankel integral, DC bias.

1 Introduction

Translated from *Journal of Nanjing University of Information Science & Technology*, 2023, 15(1): 121-126.
*Corresponding author. *Email addresses:* **lvteng320@163.com** (H. Qi).

Dc power transmission in the unipolar earth return operation mode, high amplitude direct current will flow into the earth through the DC ground pole. Due to the poor conduction of the ground and the simultaneous action of the wide-area power grid, part of the DC current will invade the AC system, resulting in an adverse effect on the transformer, that is, the DC magnetic bias hazard. Dc magnetic bias seriously endangers the safe operation of power system. The DC bias tolerance characteristics of transformers are very complex [1-3], and the control of DC bias also requires a lot of manpower and material resources [4-7].

Operation experience shows that the root cause of DC magnetic bias hazard of power grid is the uneven distribution of surface potential caused by DC grounding electrode [8-11], which is manifested as follows: transmission lines are connected to many substations that are far apart, and the neutral points of high-voltage transformers in substations are mostly directly grounded. A parallel current channel is formed between the ground and the power network. Due to the difference of surface potential between substations, part of the incoming current of the DC transmission is "extracted" from the ground to the power system. Dc current flows through the transformer winding, the transformer core is saturated and the excitation half-cycle saturation phenomenon is generated, thus forming the DC bias hazard. Dc bias hazards are mainly transformer vibration and abnormal sound, as well as local temperature rise and harmonics.

The field-circuit coupling model of DC current intrusion is adopted in the simulation evaluation of power grid magnetic bias [10], that is, the coupling between the above-ground circuit model and the underground current field. The coupling is directly manifested as the surface potential of the power station, and the greater the difference of the surface potential between the power stations, the more serious the magnetic bias. The method of solving the surface potential is related to the selected earth model. Since the earth model used for DC magnetic bias problem is the actual geoelectrical structure model, the existing grounding analysis and evaluation methods may not be applicable [11-12]. Literature [13-15] systematically uses finite element method to solve the geodetic parameters of complex structures; literature [16-17] proposes a calculation method of surface potential considering the relief of terrain; Literature [18-19] focuses on the study of surface potential under the distribution of middle-earth fault zones. These studies mainly rely on commercial finite element software, which cannot be applied to the risk assessment of power grid magnetic bias for the time being. Geng Shan et al. [20] used the mirror image method to study the surface potential distribution around the DC grounding electrode in the complex geological environment of Xinjiang, and Ma [21] conducted the sensitivity analysis of the model parameters. However, the mirror image

method still has the problems of large calculation and low accuracy, so it cannot be applied to complex geological conditions. Ma [21] systematically studied the distribution characteristics of ground potential in the vicinity of UHV DC grounding. Li Jiali et al. [22] also carried out corresponding assessment work for the location of DC grounding electrode and the risk of DC magnetic bias under complex soil structure, and they still used the complex mirror method to solve the surface potential of DC grounding electrode. Complex image algorithm is more complex and difficult, which is not conducive to popularization and application. In addition, problems of rail potential and surface potential of high-speed railway [23], corrosion diagnosis of grounding network using surface potential [24], and echo state network analysis of step voltage [25] all need to solve surface potential, but the current research mainly relies on commercial grounding analysis software CDEGS, and lacks the support of public technical means.

To sum up, the current research relies too much on commercial finite element calculation software and grounding calculation software, and there is no reliable calculation tool for use. A Chebyshev polynomial fitting algorithm is proposed to solve the problem of calculating the surface potential distribution in a wide area caused by DC ground electrode, which provides a new idea and a new method for the application of DC bias risk assessment and other engineering problems.

2 Chebyshev polynomial solution of surface potential

2.1 Basic theory of surface potential

The DC grounding electrode causes a wide range of surface potential V, which can be written as follows:

$$V(r) = \frac{\rho_1 I}{2\pi}\int_0^\infty k_1 J_0(\lambda r)\mathrm{d}\lambda, \tag{1}$$

where, r is the distance between the surface observation point and the DC grounding pole (r is much larger than the size of the DC grounding pole), ρ_1 is the resistivity of the ground at the first layer, I is the ground return current of the DC transmission system, J_0 is the first zero-order Bessel function, λ is the integral coefficient, k_1 is the equivalent resistivity function of the horizontal stratified ground structure, which can be solved by the recurrence formula:

$$k_{n-1} = \frac{1-\mu_{n-1}\exp(-2\lambda d_{n-1})}{1+\mu_{n-1}\exp(-2\lambda d_{n-1})}, \mu_{n-1} = \frac{\rho_{n-1}-\rho_n}{\rho_{n-1}+\rho_n},$$
$$\cdots$$
$$k_i = \frac{1-\mu_i\exp(-2\lambda d_{n-1})}{1+\mu_i\exp(-2\lambda d_{n-1})}, \mu_i = \frac{\rho_i-\rho_{i+1}k_{i+1}}{\rho_i+\rho_{i+1}\cdot k_{i+1}},$$

…

$$k_1 = \frac{1-\mu_1 \exp(-2\lambda d_{n-1})}{1+\mu_1 \exp(-2\lambda d_{n-1})}, \mu_1 = \frac{\rho_1-\rho_2 k_2}{\rho_1+\rho_2 k_2}, \tag{2}$$

among them, the horizontal stratified geodetic structure is shown in Figure 1, where d is the thickness of the stratification, ρ is the resistivity of the stratification, and μ_i is the reflection coefficient of the i-th stratification.

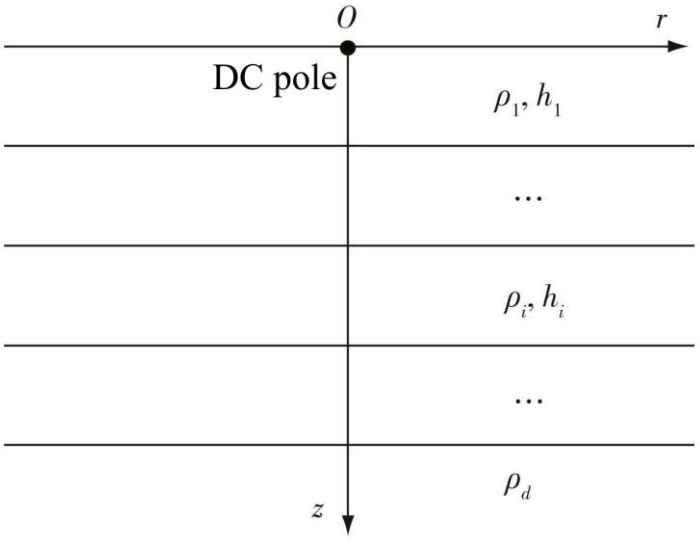

Figure 1: Horizontal stratification of the earth structure

Equation (1) belongs to the generalized infinite integral, also known as the Hankel transform, where k_1 is the integral kernel function of the Hankel transform. Because J_0 shows oscillation attenuation with the increase of $r\lambda$, the traditional numerical calculation method cannot accurately solve equation (1). If k_1 can be expanded by an infinite exponential series, then formula (1) can be solved using the classical image method, but it cannot be solved for the case of more layers. The main reason is that the theoretical expression of infinite exponential series of k_1 with more layers is too complicated and the calculation time is too long to be used in practice.

Formula (1) is the case that the source points of the field are all on the surface. For the case of any position of the field source point, it is only necessary to replace the $V(r)$ integral with the actual case, as detailed in reference [11-12].

2.2 Chebyshev polynomial solution method

The Chebyshev polynomial is a solution to the following second-order differential equation:

$$(1-x^2)\frac{\mathrm{d}^2 y}{\mathrm{d}x^2} - x\frac{\mathrm{d}y}{\mathrm{d}x} + n^2 y^2 = 0. \tag{3}$$

This paper is based on the first class of Chebyshev polynomials. The first Chebyshev polynomial T:

$$T_0(x) = 1 \tag{4}$$

$$T_n(x) = 2^{n-1}\sum_{k=0}^{[0.5n]}(-1)^n \frac{(n-k-1)!}{k!2^{2k}(n-2k)!}x^{n-2k}, \tag{5}$$

where $[0.5n]$ indicates that $0.5n$ is rounded down.

If $f(x)$ is a continuous function in the interval $[-1,1]$, it can be converted to an infinite series of T:

$$f(x) = 0.5c_0 + \sum_{n=1}^{\infty} c_n T_n(x), \tag{6}$$

$$c_n = \frac{2}{\pi}\int_{-1}^{0} \frac{f(x)T_n(x)}{\sqrt{1-x^2}}\mathrm{d}x, \tag{7}$$

formula (6) is also known as the Fourier-Chebyshev series expansion.

The basic idea of Chebyshev polynomial solution method is to use Chebyshev polynomial to convert the infinite integral of the surface potential into the summation of the finite length Chebyshev sequence, and then quickly evaluate the surface potential. The Chebyshev polynomial is solved as follows:

Step 1. Set the attenuation coefficient E of the first layer as

$$E = \exp(-2\lambda d_1). \tag{8}$$

for layer i earth, its attenuation coefficient can be rewritten as

$$E^{\delta_i} = \exp(-2\lambda d_i), \delta_i = \frac{d_i}{d_1}. \tag{9}$$

Step 2. Substitute formula (8) and (9) into formula (2) to obtain

$$k_{n-1} = \frac{1-\mu_{n-1}E^{\delta_{n-1}}}{1+\mu_{n-1}E^{\delta_{n-1}}}, \mu_{n-1} = \frac{\rho_{n-1}-\rho_n}{\rho_{n-1}+\rho_n},$$

$$\cdots$$

$$k_i = \frac{1-\mu_i E^{\delta_i}}{1+\mu_i E^{\delta_i}}, \mu_i = \frac{\rho_i - \rho_{i+1}k_{i+1}}{\rho_i + \rho_{i+1}k_{i+1}},$$

$$\cdots$$

$$k_1 = \frac{1-\mu_1 E^{\delta_1}}{1+\mu_1 E^{\delta_1}}, \mu_1 = \frac{\rho_1-\rho_2 k_2}{\rho_1+\rho_2 k_2}, \tag{10}$$

using the series expansion, the equation (10) can be reduced to

$$\frac{1-\mu_1 E^{\delta_1}}{1+\mu_1 E^{\delta_1}} \approx A_0 + A_1 E + A_2 E^2 + \cdots = \sum_{i=0}^{m} A_i E^i. \tag{11}$$

Three steps such as shift operation, coefficient expansion and truncation error determination are introduced to solve equation (11).

1) **Shift operation**

The range of the Chebyshev polynomial is $[-1,1]$, while the coefficient k_1 is $[0,1]$. Therefore, the Chebyshev polynomial must be shifted, and the shift Chebyshev polynomial T_j expression is

$$
\begin{aligned}
&T_0(E) = 1,\\
&T_1(E) = 2E - 1,\\
&T_2(E) = 8E^2 - 8E + 1,\\
&T_3(E) = 32E^3 - 48E^2 + 18E - 1,\\
&T_4(E) = 128E^4 - 256E^3 + 160E^2 - 32E + 1,\\
&\cdots\\
&T_{m+1}(E) = 2 \cdot (2E - 1) \cdot T_m(E) - T_{m-1}(E), m \geq 1.
\end{aligned} \tag{12}
$$

2) **Coefficient expansion**

Carry out the shifted Chebyshev polynomial expansion of k_1, and equation (11) is converted to

$$k_1(E) \approx -0.5c_0 + \sum_{k=0}^{n} c_k T_k(E) \to A_0 + A_1 E + A_2 E^2 + \cdots, \tag{13}$$

where, c_j is the coefficient of T_j, and the specific expression of c_j is

$$c_j = \frac{2}{m} \sum_{b=0}^{m} k_1(\xi_b) \cos\left(\pi j \frac{b+0.5}{m+1}\right), \tag{14}$$

where, ξ_b is the root of T_b coefficient equation, and the specific expression of ξ_b is

$$\xi_b = 0.5 + 0.5 \cos\left(\pi \frac{b+0.5}{m+1}\right), b = 0,1,\cdots,m. \tag{15}$$

3) **Truncation error determination**

The error expression of m-order shift Chebyshev polynomial expression can be written as

$$\varepsilon_m(E) = \sum_{b=m+1}^{\infty} c_b T_b(E). \tag{16}$$

equation (16) approximates the error principal term:

$$\varepsilon_m(E) \approx c_{m+1} T_{m+1}(E), \tag{17}$$

the total error of the E range error is

$$\varepsilon_{\text{tot}} \approx \int_0^1 c_{b+1} T_{b+1}(E) dE, \tag{18}$$

the theoretical result of the integral of equation (18) is

$$\varepsilon_{\text{tot}} \approx \frac{2}{m+1} \sum_{b=0}^{m+1} k_1(\xi_b) \cos\left(\frac{\pi(b+0.5)(m+1)}{m+2}\right) \cdot \sum_{i=0}^{m+1} \frac{t_i}{i+1}, \tag{19}$$

where t_i is the coefficient of the shifted Chebyshev polynomial in equation (12).

Therefore, the highest order m in equation (13) can be determined according to the process shown in Figure 2.

Step 3. Substitute equation (11) into equation (1)

$$V(r) = \frac{\rho_1 I}{2\pi} \int_0^{\infty} \sum_{i=0}^{n} A_i E^i J_0(\lambda r)\, \mathrm{d}\lambda. \tag{20}$$

According to the Lipschitz integral formula

$$\int_0^{\infty} \exp(-\lambda|x|) J_0(\lambda y) \mathrm{d}\lambda = \frac{1}{\sqrt{x^2+y^2}}, \tag{21}$$

If you put in equation (20), there is

$$V(r) = \frac{\rho_1 I}{2\pi}\int_0^{\infty}\sum_{i=0}^{n} A_i E^i J_0(\lambda r)\,\mathrm{d}\lambda = \frac{\rho_1 I}{2\pi}\sum_{i=0}^{n}\frac{A_i}{\sqrt{4i^2 d_1^2 + r^2}}. \tag{22}$$

input current I, solve equation (22), output the calculation result.

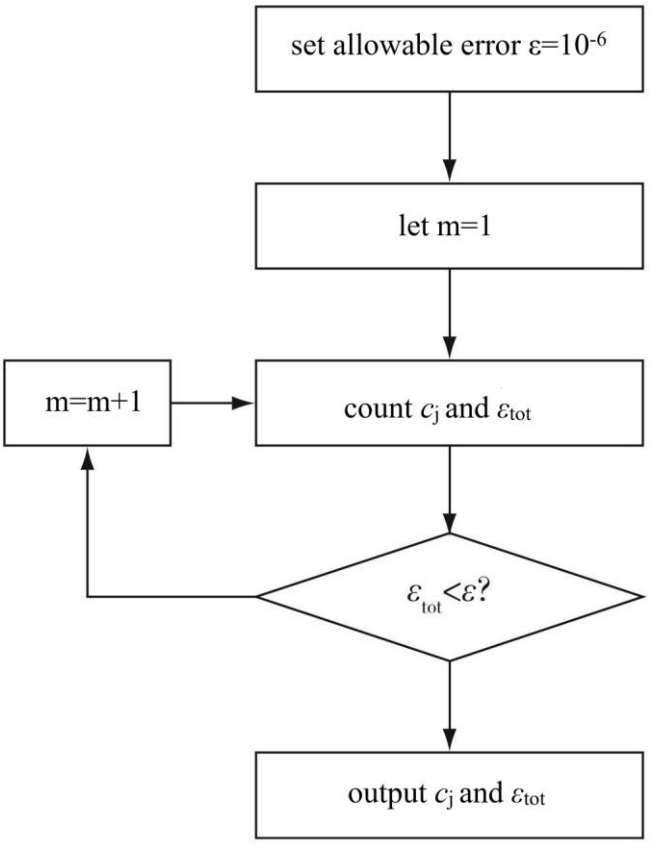

Figure 2: Flowchart to determine the maximal order m for the shift Chebyshev polynomial

The Chebyshev polynomial method greatly reduces the difficulty of calculating the surface potential distribution caused by the ground return current of HVDC transmission, and helps to form the calculation software.

3 Analysis and comparison of numerical examples

The calculation result of standard grounding calculation software CDEGS on the potential of 5 000 A point current source at the surface range of $1-100$ km is introduced and compared with the 20-order Chebyshev polynomial method. The surface potential distribution of the two different methods is shown in Figure 3. The deviation between the proposed method and the calculated results of CDEGS is 0.71 V at 1 km, 0.13 V at 10 km, and 0.04 V at 100 km.

Table 1: Horizontal8-layer structure geometric parameters

layer number	resistivity/(Ω·m)	thickness/m
1	15	300
2	45	2 250
3	200	3 000
4	2 000	5 000
5	5 000	29 500
6	3 000	15 000
7	50	20 000
8	882	Infinity

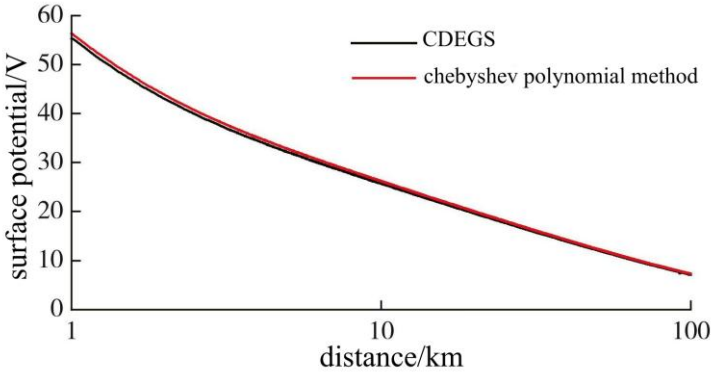

Figure 3: Comparison between the 20th-order Chebyshev polynomial method and CDEGS software

Since the calculation accuracy and convergence speed of Chebyshev polynomial method are closely related to the order, the results of surface potential at different observation points of the soil model in Table 1 under different order are given in Table 2. As can be seen from the results in Table 2, when the order is 10, the calculation results have a large deviation, but when the order reaches 20 or above, the calculation results tend to be stable. In the range of 1-100 km, even the 20-order Chebyshev polynomial method has reached sufficient accuracy for engineering applications.

In order to further analyze the numerical differences in Table 2, this paper conducted a more in-depth calculation analysis of Chebyshev polynomial fitting error equation (19) based on the situation in Table 1, and the results were shown in Table 3. As can be seen from Table 3, at the beginning, with the increase of the order of Chebyshev polynomials, the theoretical deviation of kernel function fitting decreases rapidly, but when the order reaches 20, the convergence rate tends to slow down. The application of this paper shows that as long as the order of Chebyshev polynomial is selected as the error is small, it can

achieve a better engineering application effect, and the calculation speed is faster. Blindly increasing the order cannot bring obvious accuracy improvement to the calculation result, but will waste a lot of calculation time.

Table 2: Surface potential calculated by Chebyshev polynomial method with different orders

V

distance/m	Chebyshev polynomial order m				
	10	20	30	40	50
1	4 902. 02	3 796. 73	3 828. 96	3 820. 51	3 820. 43
2	3 865. 30	3 339. 97	3 365. 37	3 362. 12	3 361. 48
3	3 053. 36	2 846. 21	2 868. 55	2 866. 50	2 866. 52
4	2 494. 21	2 422. 13	2 442. 53	2 441. 20	2 441. 30
5	2 095. 35	2 083. 65	2 102. 40	2 101. 49	2 101. 48
6	1 800. 18	1 817. 42	1 834. 75	1 834. 02	1 833. 92
7	1 574. 63	1 606. 62	1 622. 75	1 622. 08	1 621. 94
8	1 397. 51	1 437. 42	1 452. 50	1 451. 87	1 451. 73
9	1 255. 16	1 299. 54	1 313. 68	1 313. 08	1 312. 95
10	1 138. 51	1 185. 49	1 198. 79	1 198. 22	1 198. 12
1 000	42. 29	56. 23	56. 38	56. 36	56. 37
10 000	32. 79	26. 18	26. 19	26. 19	26. 19
100 000	6. 37	7. 28	7. 28	7. 28	7. 28

Table 3: Fitting error of Chebyshev polynomial method with different orders

chebyshev polynomial order m	theoretical deviation of formula (19)/V
10	1. 860
20	0. 061
30	0. 036
40	0. 031
50	0. 030

4 Conclusions

In order to solve the problem of surface potential distribution caused by DC ground

electrode, a method of solving the integral kernel function of Hankel transform fitting the surface potential by Chebyshev polynomial is proposed.

1) The Fourier-Chebyshev series expansion of the basic integral kernel function is solved by introducing three aspects, such as shift operation, coefficient expansion and truncation error determination, and the Chebyshev polynomial adaptive order fitting method of the kernel function is obtained, thus greatly reducing the difficulty of calculating the surface potential distribution.

2) The effect of the order m of Chebyshev polynomial on the calculation result is analyzed by using a geodetic example of horizontal 8-layer structure. The results show that when the distance between field point and source point is less than 10 m, the order of Chebyshev polynomial needs to be 40, and when the distance between field point and source point is greater than 1 km, the order of 20 can meet the accuracy requirements. The accuracy of the proposed method is verified by comparing it with the reference grounding software CDEGS.

3) The surface potential solution method based on shifted Chebyshev polynomials provides a basic technical means for DC magnetic bias risk assessment, helps to reduce the difficulty of DC magnetic bias risk assessment of power grid, assists DC magnetic bias risk assessment and other related work, and can provide relevant technical support for power system grounding design and other industries.

Acknowledgments

This work is supported by the National Natural Science Foundation of China (Grant No. 51607129).

Conflicts of Interest

The authors declare no conflict of interest.

References

[1] Z. Z. Wang, K. Liu, M. Y. Li, et al., Co-simulation and analysis of "three transformers" for UHV transformer under DC-bias, *High Volt. Eng.*, 2020, 46(12): 4097-4105.

[2] M. S. Guo, A consideration of allowable DC bias current of large power transformers, *Transformer*, 2021, 58(3): 15-21.

[3] M. Y. Li, J. S. Zhang, H. M. Li, et al., Loss and temperature rise test and analysis on 500 kV single-phase auto-transformer under no-load DC bias, *High Volt. Appar.*, 2021, 57(6): 132-139.
[4] Z. R. Rong, S. M. Ma, X. N. Lin, et al., Suppression strategy of DC bias based on coordination between grounding electrodes interconnecting and DC blocking devices, *Power Syst. Technol.*, 2021, 45(9): 3453-3462.
[5] Z. H. Pan, X. M. Wang, B. Tan, et al., Potential compensation method for restraining the DC bias of transformers during HVDC monopolar operation, *IEEE Trans. Power Deliv.*, 2016, 31(1): 103-111.
[6] Z. C. Xie, X. N. Lin, Z. Y. Zhang, et al., Advanced DC bias suppression strategy based on finite DC blocking devices, *IEEE Trans. Power Deliv.*, 2017, 32(6): 2500-2509.
[7] Z. X. Wang, Z. C. Xie, C. Liu, et al., Novel DC bias suppression device based on adjustable parallel resistances, *IEEE Trans. Power Deliv.*, 2018, 33(4): 1787-1797.
[8] L. G. Liu, and C. L. Ma, Calculation of multi-layer soil earth surface potential distribution of HVDC due to finite element method, *Power Syst. Prot. Control*, 2015, 43(18): 1-5.
[9] Z. X. Fu, H. D. Tan, H. F. Liu, et al., Potential numerical simulation and analysis of influencing factors of toroidal HVDC grounding electrode, *Power Syst. Technol.*, 2016, 40(6): 1909-1915.
[10] Z. H. Pan, L. Zhang, X. M. Wang, et al., HVDC ground return current modeling in AC systems considering mutual resistances, *IEEE Trans. Power Deliv.*, 2016, 31(1): 165-173.
[11] W. Li, Z. H. Pan, H. L. Lu, et al., Influence of deep earth resistivity on HVDC ground-return currents distribution, *IEEE Trans. Power Deliv.*, 2017, 32(4): 1844-1851.
[12] Z. H. Pan, J. S. Li, Y. J. Liu, et al., Multi-precision-resolution computation of the Green's function for the grounding problems of layered soils, *Proc. CSEE*, 2019, 39(15): 4451-4459.
[13] C. L. Ma, L. G. Liu, L. T. Wang, et al., The ANSYS simulation of HVDC grounding electrode potential distribution, *Adv. Power Syst. Hydroelectr. Eng.*, 2017, 33(4): 19-26, 33.
[14] L. G. Liu, K. R. Jiang, Y. Li, et al., Three-dimensional earth resistivity structure modelling around DC ground electrode, *Proc. CSEE*, 2018, 38(6): 1622-1630.
[15] J. L. Li, C. C. Li, and P. Feng, Analysis of the influence of complex soil structure on DC current flowing into transformer, *Insul. Surge Arresters*, 2020(3): 34-42.
[16] W. X. Sima, D. H. Luo, T. Yuan, et al., Influence of vertical drop of soil on grounding resistance measurement of grounding grid and the improvement measures, *High Volt. Eng.*, 2018, 44(5): 1490-1498.
[17] Q. Xiong, M. X. Wang, H. Huang, et al., Establishment of earth model for HVDC earth electrode in complicated terrain, *Proc. CSEE*, 2020, 40(7): 2269-2277.
[18] M. W. Guo, Y. F. Fan, S. Geng, et al., Study on the effect of fracture structure adjacent to ground electrodes of UHVDC power transmission lines on earth surface potential distribution, *Power Syst. Prot. Control*, 2019, 47(2): 73-79.
[19] J. L. Li, C. C. Li, and P. Feng, Analysis of layered soil resistance effect on HVDC grounding diffuser performance, *Insul. Surge Arresters*, 2020(2): 1-9.
[20] S. Geng, Y. F. Fan, X. L. Gong, et al., Calculation of earth surface potential around UHVDC grounding electrode and analysis on sensitive parameters, *High Volt. Appar.*, 2019, 55(3): 163-169.
[21] C. L. Ma, Research on distribution characteristics of earth potential near UHVDC grounding electrode, Beijing: North China Electric Power University, 2020.
[22] J. S. Li, Y. J. Liu, Z. H. Pan, et al., Site selection of DC grounding electrodes in complex soil and risk assessment of DC bias, *Electr. Meas. Instrum.*, 2021, 58(2): 13-18.
[23] A. H. Xiong, Analysis of rail potential and surface potential of integrated grounding system

in different sections of high-speed railway, Chengdu: Southwest Jiaotong University, 2017.
[24] F. H. Wang, S. J. Wang, Y. D. Liu, et al., Comparison of substation grounding grid fault diagnosis results using surface potential and magnetic induction intensity, *High Volt. Eng.*, 2016, 42(7): 2281-2289.
[25] Q. Sheng, F. H. Wang, L. J. Sheng, et al., Calculation of surface potential distribution of grounding grid based on echo state network, *High Volt. Appar.*, 2019, 55(3): 144-149.